

# Gaussian distribution of inhomogeneous barrier height in tungsten/4H-SiC (000-1) Schottky diodes

S. Toumi<sup>a</sup>, A. Ferhat-Hamida<sup>a</sup>, L. Boussouar<sup>a</sup>, A. Sellai<sup>b</sup>, Z. Ouennoughi<sup>a,\*</sup>, H. Ryssel<sup>c</sup>

<sup>a</sup> Laboratoire optoélectronique et composants, Physics Department, Sétif Algeria, Algeria

<sup>b</sup> Physics Department, P.O. Box 36, Sultan Qaboos University 123, Oman

<sup>c</sup> University Erlangen-Nurnberg, Chair of Electron Devices, Cauerstrasse 6, 91058 Erlangen, Germany

## ARTICLE INFO

### Article history:

Received 4 June 2008

Received in revised form 12 September 2008

Accepted 10 October 2008

Available online 5 November 2008

### Keywords:

Electrical measurements

Schottky barrier

Silicon carbide

Tungsten

Inhomogeneity

## ABSTRACT

The Gaussian distribution model have been used to analyze the anomalies observed in tungsten (W)/4H-SiC current voltage characteristics due to the barrier inhomogeneities that prevail at the metal-semiconductor interface. From the analysis of the forward  $I$ - $V$  characteristics measured at elevated temperatures within the range of 303–448 K and by the assumption of a Gaussian distribution (GD) of barrier heights (BHs), a mean barrier height  $\Phi_{B0}$  of 1.277 eV, a zero-bias standard deviation  $\sigma_0 = 0.092$  V and a factor  $T_0$  of 21.69 K have been obtained. Furthermore the modified Richardson plot according to the Gaussian distribution model resulted in a mean barrier height  $\Phi_{B0}$  and a Richardson constant ( $A^*$ ) of 1.276 eV and 145 A/cm<sup>2</sup> K<sup>2</sup>, respectively. The  $A^*$  value obtained from this plot is in very close agreement with the theoretical value of 146 A/cm<sup>2</sup> K<sup>2</sup> for n-type 4H-SiC. Therefore, it has been concluded that the temperature dependence of the forward  $I$ - $V$  characteristics of the W/4H-SiC contacts can be successfully explained on the basis of a thermionic emission conduction mechanism with Gaussian distributed barriers. In addition, a comparison is made between the present results and those obtained previously assuming the pinch-off model.

© 2008 Elsevier B.V. All rights reserved.

## 1. Introduction

Silicon carbide (SiC) is an attractive material for high power and high temperature applications because of its electrical properties such as wide band gap, excellent thermal conductivity and high breakdown electric fields [1–7]. Remarkable advances have been accomplished in SiC power semiconductor devices in recent years. Significant works have been done in development of SiC electronic devices and particularly Schottky contacts due to their technological importance [8–34]. While SiC Schottky diodes are now readily available in the market, studies related to their properties and applications remain important topics in today's research. Many authors have investigated the properties of silicon carbide Schottky rectifiers on both 6H-SiC [1–10] and 4H-SiC [11–27]. Of these two polytypes, 4H-SiC is emerging as the material of preference due to the more isotropic nature of many of its electrical properties together with high electron mobility [28,29].

Although, most of the devices are usually made using Si-face 4H-SiC substrates due to good surface morphology and the possibility of having low doping concentrations required for high power applications, C-face 4H-SiC has been recently the focus of much attention due to its different properties. The advantages of C-face

4H-SiC include high channel mobility, low leakage current and low dislocation densities. C-face has also shown to be more suitable for epitaxial growth on low off-cut angle or on-axis substrates [30–35]. It has been reported, in the same context, that the Schottky contact on the C-face crystal gives, in general, a significantly higher barrier height compared to Si-face contacts [6,11,36].

Furthermore, a number of metals such as nickel (Ni), titanium (Ti), gold (Au) and molybdenum (Mo) have been considered and studied for the formation of Metal/SiC Schottky contacts. Tungsten on SiC, however, is a less studied system and the Schottky contacts W/SiC have received limited attention [17,18,37]. Tungsten as a refractory metal has excellent advantages such as high thermal conductivity, low coefficient of thermal expansion, low specific heat, excellent thermal fatigue properties, chemical stability and high resistance to heat [38–40].

Several studies concerning electrical transport in SiC Schottky contacts have been carried out during the last decades. The current transport and the temperature dependence of the Schottky barrier height (SBH) in SiC Schottky diodes remain a topic of current interest.

Experimental  $I$ - $V$ - $T$  data obtained from many different Schottky diodes often exhibit non-ideal  $I$ - $V$ - $T$  characteristics and reveal abnormal variations of barrier height ( $\Phi_B$ ) and ideality factor ( $n$ ) with temperature. These variations are usually interpreted by the existence of inhomogeneities at the interface which might be

\* Corresponding author. Tel.: +213 776317925; fax: +213 36937943.

E-mail address: [ouennoughi@gmail.com](mailto:ouennoughi@gmail.com) (Z. Ouennoughi).

caused by several physical reasons like doping inhomogeneity, contamination at the interface causing high interface state density, defects, mixture of different phases, etc. [14,41,42]. Moreover, many experimental studies confirm that the SBH is non-uniform.

Two approaches are generally proposed in the literature to explain the experimental data and model the current–voltage–temperature ( $I$ – $V$ – $T$ ) characteristics of inhomogeneous Schottky barrier contacts. These are based, namely, on models proposed by Tung [43] and Werner and Guttler [42]. The two approaches have been more or less successfully used in the interpretation of experimental results on various practical SiC Schottky diodes [9,10,19–21,27,44,45].

To explain departures from ideality, Tung [43] considers in his model the presence of locally non-uniform regions or patches with relatively lower or higher barriers with respect to an average barrier height. The interaction of the high barrier and low barrier is described with the help of the so called “saddle point”. However, in Werner’s model [42], the BH is supposed to be distributed according to a Gaussian type function which will usually lead to an apparent BH that is both temperature and bias dependent.

In the present paper, we analyse the forward  $I$ – $V$ – $T$  characteristics of the system W/4H-SiC within the framework of Werner’s Model, under the assumption of a Gaussian distribution of the barrier height, to yield information pertinent to the Schottky diode parameters and interpret their dependence on temperature. Additionally, the results obtained here are compared with those obtained recently [27] on the same device using Tung’s approach. We attempt to discuss the relationship between the two approaches.

## 2. Device fabrication and characterisation

Briefly, the substrate material used for the Schottky diodes was n-type 4H-SiC (0001), Si-face 8° off-oriented toward  $\langle 11\bar{2}0 \rangle$ , from Cree Inc. The wafers had a n-type epitaxial-layer with a donor concentration in the range of  $8.0 \times 10^{15} \text{ cm}^{-3}$  to  $1.3 \times 10^{16} \text{ cm}^{-3}$ . A 42 nm thick oxide layer is thermally grown on the epitaxial-layer served both as passivation layer for regions around the Schottky contact and as a sacrificial layer for regions where the contacts were formed. The ion implantation of aluminium at different energies and doses for the formation of the guard rings was done at room temperature using a Varian 350D ion implanter.

The Schottky contacts had a circular geometry with a diameter of 200  $\mu\text{m}$ . Schottky contacts were formed by depositing, through e-beam evaporation, tungsten on the SiC substrate at a pressure of approximately  $1 \times 10^{-5} \text{ Pa}$  followed by annealing in an open furnace at 500 °C under a  $\text{N}_2$  flow of about 1000 sccm. The structure of a fabricated SBD device is shown in Fig. 1. Further details concerning the fabrication of the W/4H-SiC Schottky diodes were given in Ref. [18].

The  $I$ – $V$  measurements were performed with a Keithley 237 Source and Measurement Unit which is capable of handling voltages up to 1100 V. The electrical IV measurements of the Schottky diodes were made in the temperature range of 303–448 K with a step of 25 K. It has to be noted that that in our  $I$ – $V$ – $T$  measurements the typical reading error in the current is less than 1% and the temperature is determined with accuracy better than 0.1 K.

## 3. Results and discussion

### 3.1. Standard theory

$I$ – $V$ – $T$  measurements are usually used in order to identify the different conduction mechanisms in current transport. At first, we consider the thermionic emission–diffusion (TED) theory which we will later modify to account for the Gaussian distribution of the

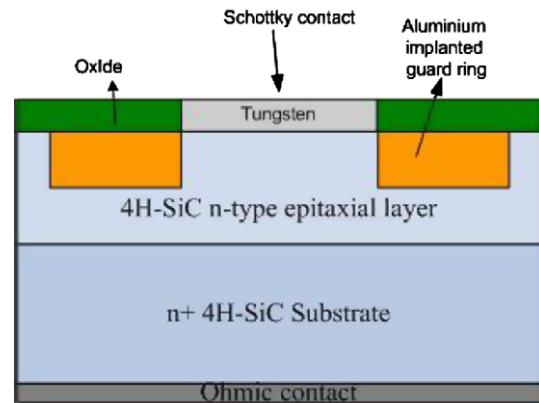


Fig. 1. The cross-sectional diagram of fabricated W/4H-SiC SBD.

barrier. Fig. 2 shows the forward  $I$ – $V$ – $T$  characteristics of the W/4H-SiC SBD measured at temperatures 303–448 K range.

The current through a homogeneous SBD at a forward bias  $V$  is described within the TED theory [46] by

$$I = I_s [\exp(\frac{\beta}{n}(V - R_s I)) - 1] \quad (1)$$

with the saturation current  $I_s$  defined by

$$I_s = AA^* T^2 \exp(-\beta \Phi_{B0}), \quad (2)$$

where  $\beta = q/kT$  is the inverse thermal voltage,  $A$  the diode area,  $k$  the Boltzmann constant and  $T$  the temperature.

A computer program is used to determine the parameters of Schottky barrier diodes (SBDs) such as the zero-bias Schottky barrier height (SBH)  $\Phi_{B0}$ , deduced from Eq. (2)  $\Phi_{B0} = -\ln(I_s/AA^* T^2)/\beta$ , the ideality factor  $n$  and the series resistance  $R_s$  associated with the bulk material in the semiconductor and the back ohmic contact.

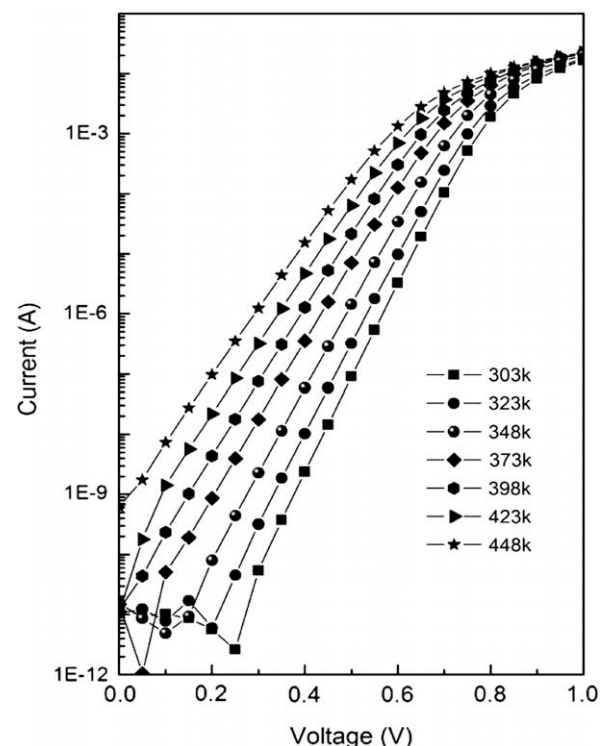


Fig. 2. Experimental forward  $I$ – $V$  curves of W/4H-SiC(000-1) diode at different temperatures.

Fig. 3 shows the experimental values of  $n$  (indicated in open triangles) and  $\Phi_{B0}$  (indicated by filled triangles) as a function of temperature. The theoretical value of the Richardson constant  $A^*$  for 4H-SiC was taken as  $146 \text{ A/cm}^2 \text{ K}^2$  [47].

The experimental value of  $n$  increases with a decrease in temperature and the value of  $\Phi_{B0}$  decreases with a decrease in temperature ( $\Phi_{B0} = 1.113 \text{ eV}$  at  $T = 303 \text{ K}$  and  $\Phi_{B0} = 1.167 \text{ eV}$  at  $T = 448 \text{ K}$ ).

The temperature dependence of the series resistance extracted from our curves is shown in Fig. 4. The series resistance increase with increasing temperature as could be expected for semiconductors in the temperature region where there is no carrier freezing out which is non-negligible only below  $\sim 100 \text{ K}$  [48]. A similar temperature dependence was obtained theoretically by Osvald and Horv  th [49] and experimentally for the epitaxial-layer of a Ti/4H-SiC diode [50].

The conventional Richardson's plot shown in Fig. 5 (indicated in filled squares) of the  $\ln(I_s/T^2)$  as a function of inverse temperature ( $\ln(I_s/T^2) = \ln(AA^*) - (q/kT)\Phi_B^{\text{eff}}$ ) is usually used to determine the effective BH and the Richardson's constant. It is clearly manifest from Fig. 5 that the experimental data can be fitted perfectly by a straight line. The value of the Richardson's constant was found from the y-intercept to be  $1.98 \text{ A/cm}^2 \text{ K}^2$ . The effective BH,  $\Phi_B^{\text{eff}}$  was found from the slope of the curve to be  $1.004 \text{ eV}$ . The extracted value of the Richardson's constant has been found to be almost two orders of magnitude lower than the theoretically predicted value ( $146 \text{ A/cm}^2 \text{ K}^2$ ). The smaller value of  $A^*$  indicates that the effective active area is in fact much smaller than the device area. These results do not agree with pure thermionic emission model.

### 3.2. The barrier height inhomogeneity

Analysis of the  $I$ - $V$  characteristics of SBDs based on TED theory reveals usually an abnormal decrease in the BH and an increase in the ideality factor with a decrease in temperature.

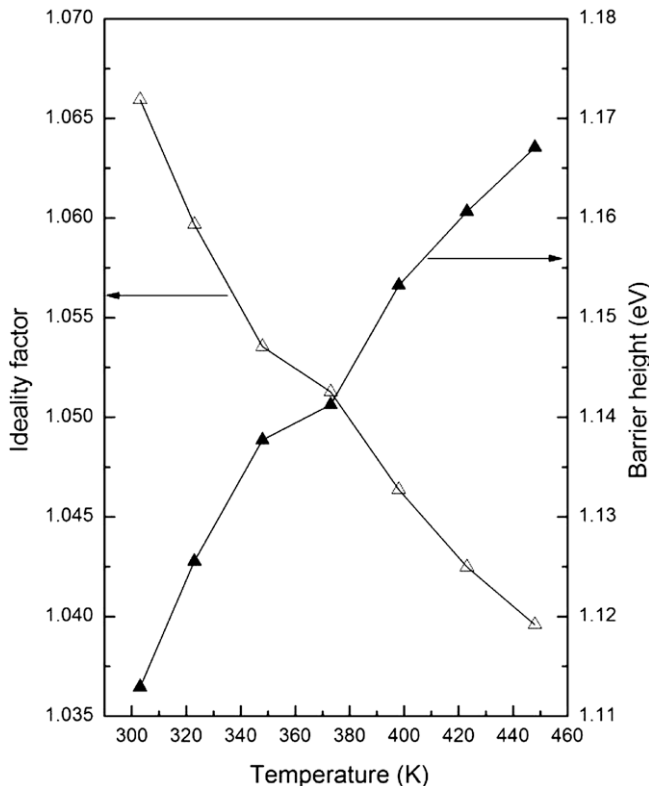


Fig. 3. SBH (filled triangles), ideality factor (open triangles) as a function of the absolute temperature for W/4H-SiC diode.

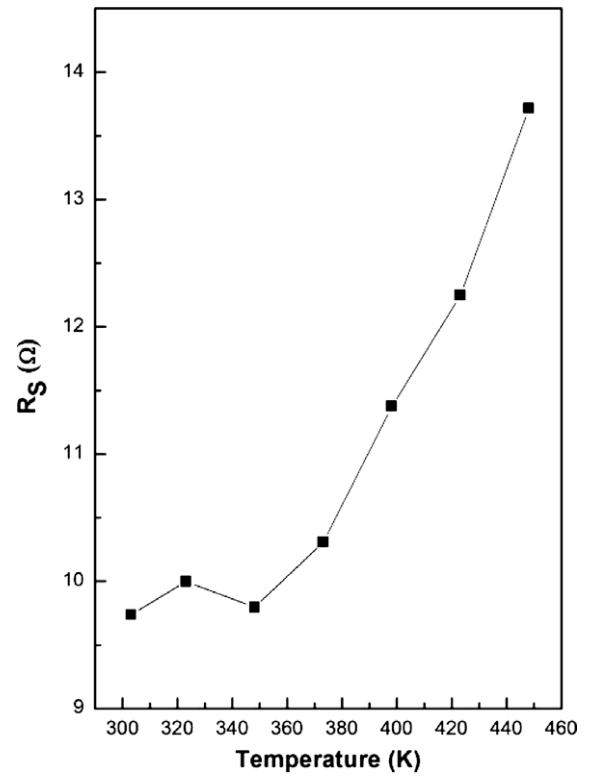


Fig. 4. The temperature dependence of the series resistance.

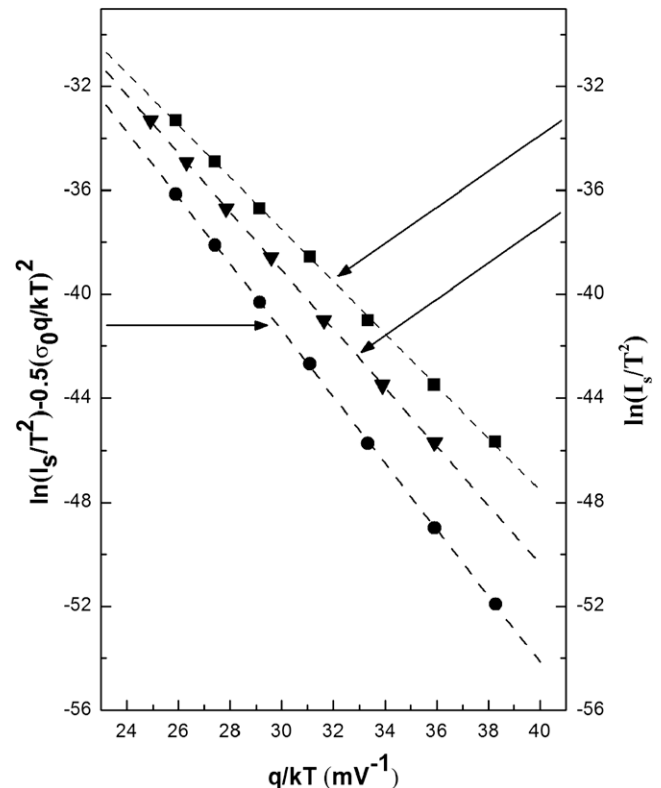


Fig. 5. Conventional Richardson plot of the  $\ln(I_s/T^2)$  vs  $(q/kT)$  (filled squares), modified Richardson plot (filled triangles) and the modified  $\ln(I_s/T^2) - (q^2\sigma^2)/2k^2T^2$  vs  $q/(kT)$  (filled circles) of W/4H-SiC(000-1) diode according to Gaussian distribution.

Lately, the nature and origin of these anomalies in our previous study [27] have been successfully explained on the basis of a TED mechanism which takes into consideration the pinch-off model proposed by Tung [43].

In the present paper, we analyse the above abnormal (temperature dependence of  $n$  and  $\Phi_B$ , the smaller value of  $A^*$ ) behaviour using the Werner's Model by the assumption of a Gaussian distribution of the barrier height to determine information, i.e., inhomogeneity leading to the abnormal dependence on the temperature of the barrier height and the ideality factor.

Gaussian distribution of SBH ( $\Phi_B$ ) with a mean value of  $\bar{\Phi}_B$  and standard deviation  $\sigma$  given by

$$P(\Phi_B) = \frac{1}{\sigma\sqrt{2\pi}} \exp \left[ -\frac{(\Phi_B - \bar{\Phi}_B)^2}{2\sigma^2} \right]. \quad (3)$$

Song et al. [51] followed by Werner and Güttler [42] were the first to introduce the analytical function potential fluctuations in the TED model where the interface between the metal and the semiconductor is considered as not atomically flat but exhibits certain roughness. As a result, the built-in potential and the BH will fluctuate spatially following a specific distribution supposed generally as Gaussian.

There are several reasons, as mentioned earlier, to include barrier fluctuation into the analysis of the transport measurement on Schottky diodes like crystal defects, non-uniformity in the interfacial charges, and spatial distribution of the doping atoms.

Hence, the total junction current is the sum of currents flowing through all individual areas of spatial regions of different BHs.

The total current is then given by

$$I(V) = \int_0^\infty i(V, \Phi_B) P(\Phi_B) d\Phi_B, \quad (4)$$

where  $i(V, \Phi_B)$  is the elementary current at a bias  $V$  for a barrier of height  $\Phi_B$ , given by Eq. (1) and  $P(\Phi_B)$  is the normalized distribution function giving the probability of the occurrence of Barrier height  $\Phi_B$ .

Werner and Guttler assume a linear bias dependence of  $\bar{\Phi}_B$

$$\bar{\Phi}_B - \bar{\Phi}_{B0} = \rho_2 V \quad (5)$$

and a quadratic bias dependence of  $\sigma$  (the temperature dependence of  $\sigma$  is small and can be neglected).

$$\sigma^2 - \sigma_0^2 = \rho_3 V \quad (6)$$

The coefficients  $\rho_2$  and  $\rho_3$  are independent of temperature and quantify the voltage deformation of the barrier distribution [42].

And performing integration of Eq. (4) we obtain

$$I = I'_s \left[ \exp \left( \frac{\beta}{n_{ap}} (V - R_s I) \right) - 1 \right] \quad (7)$$

with

$$I'_s = AA^{**} T^2 \exp(-\beta \Phi_{ap}), \quad (8)$$

where

$$\Phi_{ap} = \bar{\Phi}_{B0} - \frac{\beta \sigma_0^2}{2} \quad (9)$$

and

$$\frac{1}{n_{ap}} = 1 - \rho_2 + \frac{\beta \rho_3}{2} \quad (10)$$

As Eqs. (1) and (7) are of the same form, the fitting of the experimental data to Eq. (7) gives  $\Phi_{ap}$  and  $n_{ap}$ , which should obey Eqs. (9) and (10).

Thus, the plot of  $\Phi_{ap}$  vs  $q/2kT$  (Fig. 6) should be a straight line that gives  $\bar{\Phi}_{B0} = 1.277$  eV and  $\sigma_0 = 0.092$  V from the intercept and

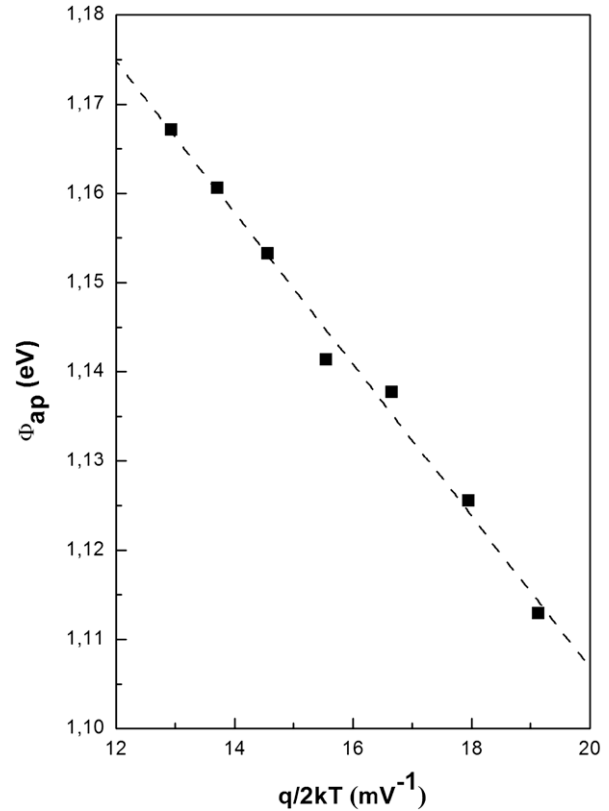


Fig. 6. Apparent barrier height vs  $q/2kT$  curve of W/4H-SiC(000-1) diode according to Gaussian distribution.

slope, respectively. The lower value of  $\sigma_0$  corresponds to more homogeneous BH. However, the value of  $\sigma_0 = 0.092$  V is not small compared to the mean value of  $\bar{\Phi}_{B0} = 1.277$  eV (7%), and it indicates the presence of the interface inhomogeneities.

This value is very close to the theoretical SBH  $\Phi_B = \Phi_m - \chi$  of about 1.25 eV expected for the W/4H-SiC SBH obtained by considering the tungsten work function,  $\Phi_m = 4.55$  eV [52], and the usually used value of the electron affinity of 4H-SiC,  $\chi = 3.3$  eV [12,53,54].

Schottky barrier height vs metal work function in metal/4H-SiC systems is plotted in Fig. 7. The barrier height for a certain metal has been taken from Refs. [11,36]. The common factor of the Schottky contacts is that they are made on the C-face of a 4H-SiC substrate. We separated data of several authors in three groups depending on the method of the measurements.

Strong Fermi-level pinning is not observed, and the barrier height depends on the metalwork function with slopes  $S$  of 0.55–0.76. Thus, according to the theory, the Fermi-level is assumed to be only partially pinned by interfacial surface states. This means that the Schottky barrier is influenced by surface states but their density  $D_s$  is not sufficient enough to totally pin the Fermi-level of the semiconductor to the surface potential  $\Phi_0$ .

The straight line in Fig. 7 is drawn with a slope of 1 starting from 3.3 eV which is the electron affinity for 4H-SiC. This is the expected barrier height if the formation of the Schottky barrier would follow the Schottky–Mott theory giving a barrier height which is the difference between the metal work function and the electron affinity of the semiconductor.

Note that the SBH value obtained using the GD model ( $\bar{\Phi}_{B0} = 1.277$  eV) is slightly greater than the value of the uniform SBH ( $\Phi_B^0 = 1.248$  eV) obtained using Tung's [43] model and the famous Schmitsdorf's plot [55] (see Fig. 5 in Ref. [27]).

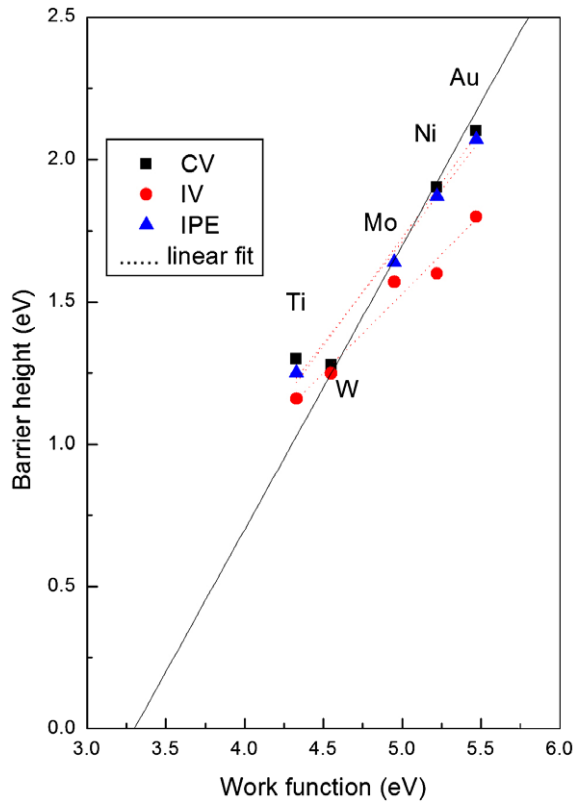


**Fig. 7.** Schottky barrier height vs metal work function for metal/4H-SiC systems. Barrier heights from capacitance-voltage (CV) and internal photoemission (IPE) measurements are obtained from Itoh et al. [11]. Barrier heights from IV measurements (except W) are obtained from Shigiltchoff et al. [36].

Even though we have not performed C-V measurements on these diodes as yet, it is expected, as it is often the case, that the barrier height from the C-V data will be closer to the average value obtained from the  $I$ - $V$ - $T$  data for the simple reason that the C-V method is insensitive to current fluctuations due to inhomogeneities. Recently, Reshanov et al. [37] have reported a SBH of W/4H-SiC value between 1.17 and 1.23 eV at 300 K determined by CV measurements at a frequency of 1 MHz. Defives et al. [16] reported a value  $\Phi_{fb}$  (flat band) of 1.27 eV on W/4H-SiC Si-face. These values are less than the SBH value obtained in our case on W/4H-SiC C-face used in our system. Note that there are differences in the barrier heights between Si- and C-faces, and the barrier heights for C-faces are in general 0.1–0.4 eV larger than those for Si-face [6,11].

Also, the  $(1/n_{ap} - 1)$  vs  $q/2kT$  plot is given in Fig. 8. According to Eq. (10), the plot should be a straight line that gives voltage coefficients  $\rho_2$  and  $\rho_3$  from the intercept and slope, respectively. The values of  $\rho_2 = -0.010$  and  $\rho_3 = -3.7$  mV were obtained from this plot.

The values obtained for  $\rho_2$  and  $\rho_3$  are in the same order of magnitude published previously on SiC diodes [10,21,24,45]. Instead of assuming a quadratic dependence of  $\sigma$ , Chand and Kumar [56,57] suggest both  $\bar{\Phi}_B$  and  $\sigma$  are linearly dependent on the voltage

$$\bar{\Phi}_B - \bar{\Phi}_{B0} = \gamma V \quad (11)$$

and

$$\sigma - \sigma_0 = \xi V \quad (12)$$

In this case we obtain the same expression for the apparent barrier height however the ideality factor is given by (with some approximations)

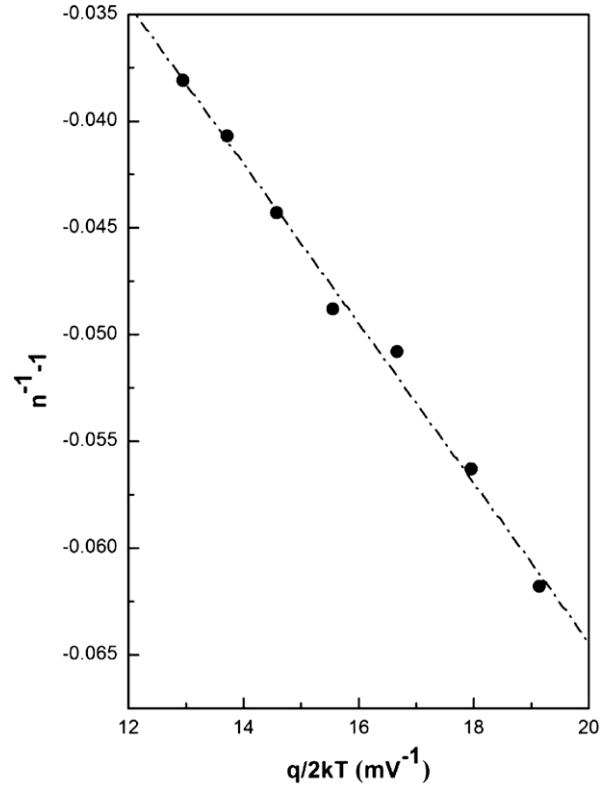


**Fig. 8.** The  $(1/n_{ap} - 1)$  vs  $q/2kT$  plot of W/4H-SiC(000-1) diode according to Gaussian distribution.

$$\frac{1}{n_{ap}} = 1 - \gamma + \frac{q\sigma_0\xi}{kT} \quad (13)$$

the  $(1/n_{ap} - 1)$  vs  $q/kT$  plot (not shown here) leads also a straight line that gives the coefficients  $\gamma$  of about 0.01 and  $\xi$  of about  $-0.02$ . The linear behaviour of the  $(1/n_{ap} - 1)$  vs  $q/2kT$  plot confirms that the ideality factor does indeed denote the voltage deformation of the Gaussian distribution of the barrier height.

According to Werner and Güttler [42] the ideality factor can be written as

$$n_{ap} \simeq 1 + \rho_2 - \frac{\rho_3}{2kT/q} \simeq 1 + \frac{T_0}{T} \quad (14)$$

which yields to (in most cases the terms  $\rho_2$  is neglected)

$$T_0 \equiv -\frac{\rho_3}{2kT/q} \quad (15)$$

The coefficient  $\rho_3$  represents the voltage equivalent of  $T_0$ . If we use the calculated value of  $\rho_3$  we obtain a  $T_0$  value of 21.69 (a same value obtained using Chand's approximation) which is close to the value of  $T_0$  calculated previously using the pinch-off model [27].

According to Saxena [58], such behaviour is typical to a SBD displaying the so called “ $T_0$  effect” which means that the ideality factor can be expressed in the form

$$n(T) = 1 + \frac{T_0}{T} \quad (16)$$

Using the pinch-off model and considering a constant value of the patch parameter  $\gamma$ , the  $IVT$  measurements has been analyzed in detail in our previous paper [27], and we will not be discussed again in this paper. Fig. 3 in Ref. [27] shows that the experimental results of  $n(T)$  fit very well with the theoretical Eq. (3) with  $T_0 = 23.92$  K. Tung [43] and Sullivan et al. [41] have shown that the “ $T_0$  effect” is typical to SBD with a distribution of barrier inhomogeneities.



If we consider the case of the pinch-off model, where an inhomogeneous barrier composed of low SBH surrounded by high SBH having a Gaussian distribution of value  $\gamma$  with a standard deviation  $\sigma_p$ , the value of the expression of the ideality factor is given by [41,43]

$$n_{ap} \simeq 1 + \frac{\beta \sigma_p^2}{3V_{bb}^{1/3} \eta^{2/3}} \simeq 1 + \frac{T_0}{T}, \quad (17)$$

$$T_0 \simeq \frac{\beta \sigma_p^2}{3V_{bb}^{1/3} \eta^{2/3}}, \quad (18)$$

where  $\eta = \epsilon_s/qN_D$ ,  $V_{bb}$  is the diffusion potential,  $\epsilon_s$  dielectric constant of the semiconductor and  $N_D$  is the donor concentration.

Using Eqs. (17) and (18) a value of  $\sigma_p = 5.91 \times 10^{-5} \text{ cm}^{2/3} \text{ V}^{1/3}$  is obtained which represent the standard deviation of the distribution of the strength parameter  $\gamma$ .

The conventional Richardson plot is modified as

$$\ln \left( \frac{I_s}{T^2} \right) - \left( \frac{q^2 \sigma_0^2}{2k^2 T^2} \right) = \ln(AA^*) - \frac{q\bar{\Phi}_{B0}}{kT}. \quad (19)$$

The  $\ln(I_s/T^2) - (q^2 \sigma_0^2)/2k^2 T^2$  vs  $q/(kT)$  according to Eq. (19) should also be a straight line with the slope and the intercept at the ordinate directly yielding the mean barrier height  $\bar{\Phi}_{B0}$  and  $A^*$ , respectively. Fig. 5 depicts this plot (curve in filled circles). It can be seen that the modified Richardson plot has quite a good linearity over the temperature range corresponding to an activation energy around  $\bar{\Phi}_{B0}$ . By the least-squares linear fitting of the data,  $\bar{\Phi}_{B0} = 1.276 \text{ eV}$  and  $A^* = 145 \text{ A K}^{-2} \text{ cm}^{-2}$  are obtained. As can be seen from the plot of  $\Phi_{ap}$  vs  $q/kT$  given in Fig. 6, this value of  $\bar{\Phi}_{B0} = 1.276 \text{ eV}$  is approximately the same as the value of  $\bar{\Phi}_{B0} = 1.277 \text{ eV}$ .

The  $A^*$  value obtained from this plot is in excellent agreement with the theoretical value of  $146 \text{ A/cm}^2 \text{ K}^2$  for n-type 4H-SiC. Plots of the conventional Richardson plot and the modified Richardson plot  $\ln(I_s/T^2)$  vs  $q/(nkT)$  are also reported in the same figure for sake of comparison. A value of  $A^* = 1.98 \text{ A K}^{-2} \text{ cm}^{-2}$  has been obtained from the conventional Richardson plot and a value of  $A^* = 16.85$  has been obtained from the modified Richardson plot  $\ln(I_s/T^2)$  vs  $(q/nkT)$ .

### 3.3. Discussion of W–SiC interface

Although the analysis of the  $I$ – $V$ – $T$  data provides an indirect evidence of barrier inhomogeneities at the W/SiC interface, the method does not directly give information on the many issues that might contribute to the degradation of the quality of the interface. The interface quality could be degraded due to the existence of a thin oxide layer, non-optimized surface preparation and cleaning prior to W deposition, process-induced contamination as well as vacuum conditions during evaporation. These are usually the critical factors for achieving a good epitaxy and common reasons for deviations from the ideal behaviour of Schottky contacts in SiC. The reaction kinetics and the phase equilibria according to thermodynamic consideration lead to different possibilities of interface reactions. So what happens at the W/SiC interface determines the electrical properties of the device.

Not too many detailed experimental studies have been previously reported on the system W/SiC. It is a fact, however, that tungsten can react with the SiC to form a silicide ( $\text{WSi}_2$ ,  $\text{W}_5\text{Si}_3$ ) when reacted with elemental Si and form a carbide ( $\text{WC}$ ,  $\text{W}_2\text{C}$ ) when reacted with elemental C [38]. In particular W reacts with SiC below 970 K by forming  $\text{WSi}_2$  and WC which are stable with SiC. At temperatures between 970 K and 2140 K, W form the metal rich silicide  $\text{W}_5\text{Si}_3$  and WC. At higher temperatures (above 2140 K) the stable carbide changes to ( $\text{W}_2\text{C}$ ) [40]. Geib et al. [38] deposited W on  $\beta$ -SiC via electron beam deposition and identified  $\text{WSi}_2$  and

WC as the resulting phases formed after annealing at 1123 K. Depositing W via d.c. sputtering onto 6H-SiC, Goesmann and Schmid-Fetzer [39] saw no reaction until an annealing temperature of 1473 K, when WC and  $\text{W}_5\text{Si}_3$  were identified. In contrast Lundberg et al. [59] used chemical vapour deposition followed by annealing up to 1073 K, and observed no reaction. Baud et al. [60] deposited W via d.c. sputtering and reported no reaction of W with  $\beta$ -SiC until 1223 K anneals. On 4H-SiC, WN has been deposited by reactive sputtering on 4H-SiC to make Schottky diodes by Noblanc et al. [61] and Kakanakova-Georgieva et al. [62]. The 1200 °C annealed W (WN)/4H-SiC structures are characterized by intense interface reactions leading to tungsten carbide and tungsten silicide formation in the contact layers. Barrier height of 0.94 eV has been measured for annealed samples up to 950 °C. High temperature thermal stability of Au/Ti/WSi<sub>x</sub> Schottky contacts on 4H-SiC have been observed by Kim et al. [63]. The contacts show a maximum Schottky barrier height of 1.15 eV at an annealing temperature of 500 °C. The barrier height decreased for anneals above 600 °C. Sputter-deposited WSi<sub>x</sub> Schottky contacts on n-type 4H-SiC were also characterized as a function of annealing and measuremental temperature by Kim et al. [64]. The diodes have produced a maximum barrier height of 1.15 eV after a 500 °C annealing which appears to be the optimum condition to maximizing the barrier height. The contacts were unstable after annealing above ~700 °C.

To sum up, these studies show that the final phases that form depend on the method of metal deposition as well as the temperature of annealing. On the basis of the results presented in this paper, we believe that the reaction mechanism in our W/4H-SiC Schottky contacts formed by depositing, through e-beam evaporation, tungsten on the SiC substrate and annealed at 500 °C as described in Section 2 lead to a formation of a silicide. The relatively high barrier height obtained in this work can be explained by the Aluminium implanted guard rings used and the C-face terminated of the 4H-SiC substrates.

## 4. Conclusion

In the present work we have analysed measured  $I$ – $V$ – $T$  characteristics at elevated temperature from W/4H-SiC diodes using the Werner's Model under the assumption of a Gaussian distribution of the barrier height yield an average laterally homogeneous BH value of 1.276 eV and a standard deviation  $\sigma_0 = 0.092$ . The experimental results of  $n(T)$  fit very well with the theoretical well known equation  $n = 1 + T/T_0$  and a value of  $T_0 = 23.92 \text{ K}$  was found in good agreement with Tung's model. The unexpectedly low Richardson's constant obtained, and the SBH linear correlation with ideality factor has been attributed to inhomogeneities that prevail at the metal–semiconductor interface. The corrected value of the Richardson's constant was found to be in excellent agreement with theory.

By using metals with different work functions, the index of interfacial behaviour  $S$  was between 0.55 and 0.76. The study also provides some insight into the complicated reaction mechanisms of the W/SiC system. The results presented in this work can be useful to better understand the electrical properties in Schottky contacts for 4H-SiC devices.

## Acknowledgment

Dr. Z. Ouennoughi is supported by the Algerian ministry of research (MESRS) for an academic year in SQU.

## References

- [1] J.R. Waldrop, R.W. Grant, Appl. Phys. Lett. 62 (1993) 2685.
- [2] A.L. Syrkin, A.N. Andreev, A.A. Lebedev, M.G. Rastegaeva, V.E. Chelnokov, J. Appl. Phys. 78 (1995) 5511.

- [3] V. Saxena, J.N. Su, A.J. Steckl, IEEE Trans. Electron Dev. 46 (1999) 456.
- [4] C. Fröjd, G. Thungström, H.-E. Nilsson, C.S. Petersson, Phys. Scripta T79 (1999) 297.
- [5] C. Raynaud, K. Isoird, M. Lazar, C.M. Johnson, N. Wright, J. Appl. Phys. 91 (2002) 9841.
- [6] M.O. Aboelfotoh, C. Fröjd, C.S. Petersson, Phys. Rev. B 67 (2003) 075312.
- [7] F. Roccaforte, F. La Via, A. Baeri, F. Roccaforte, V. Raineri, L. Calcagno, F. Mangano, J. Appl. Phys. 96 (2004) 4313.
- [8] A. Venter, M.E. Samiji, A.W.R. Leitch, Phys. Stat. Sol. (c) 1 (2004) 2264.
- [9] S. Duman, S. Doğan, B. Gürbulak, A. Türit, Appl. Phys. A: Mater. Sci. Process. 91 (2008) 337.
- [10] A. Sefaoglu, S. Duman, S. Doğan, B. Gürbulak, S. Tüzemen, A. Türit, Microelectron. Eng. 85 (2008) 631.
- [11] A. Itoh, H. Matsunami, Phys. Stat. Sol. (a) 162 (1997) 389.
- [12] R. Yakimova, C. Hemmingsson, M.F. Macmillan, T. Yakimov, E. Janzén, J. Electron. Mater. 27 (1998) 871.
- [13] Q. Wahab, T. Kimoto, A. Ellison, C. Hallin, M. Tuominen, R. Yakimova, A. Henry, J.P. Bergman, E. Janzén, Appl. Phys. Lett. 72 (1998) 445.
- [14] D. Defives, O. Noblanc, C. Dua, C. Brylinski, M. Bartula, V. Aubry-Fortuna, F. Meyer, IEEE Trans. Electron Dev. 46 (1999) 449.
- [15] B.J. Skromme, E. Luckowski, K. Moore, M. Bhatnagar, C.E. Weitzel, T. Gehoski, D. Ganser, J. Electron. Mater. 29 (2000) 376.
- [16] D. Defives, O. Durand, F. Wyczisk, O. Noblanc, C. Brylinski, F. Meyer, Microelectron. Eng. 55 (2001) 369.
- [17] M. Treu, R. Rupp, H. Kapels, W. Bartsch, Mater. Sci. Forum 353–356 (2001) 679.
- [18] R. Weiss, L. Frey, H. Ryssel, Appl. Surf. Sci. 184 (2001) 413.
- [19] F. Roccaforte, F. La Via, V. Raineri, R. Pierobon, E. Zanoni, J. Appl. Phys. 93 (2003) 9137.
- [20] R. Pérez, N. Mestres, J. Montserrat, D. Tournier, P. Godignon, Phys. Stat. Sol. (a) 202 (2005) 692.
- [21] J.M. Bluet, D. Ziane, G. Guillot, D. Tournier, P. Brosselard, J. Montserrat, P. Godignon, Superlattices Microstruct. 40 (2006) 399.
- [22] X. Ma, P. Sadagopan, T.S. Sudarshan, Phys. Stat. Sol. (a) 203 (2006) 643.
- [23] C.F. Pirri, S. Ferrero, L. Scaltrito, D. Perrone, S. Guastella, M. Furno, G. Richieri, L. Merlin, Microelectron. Eng. 83 (2006) 86.
- [24] M.E. Aydın, N. Yıldırım, A. Türit, J. Appl. Phys. 102 (2007) 043701.
- [25] D.J. Ewing, Q. Wahab, R.R. Ciechonski, M. Syvajarvi, R. Yakimova, L.M. Porter, Semicond. Sci. Technol. 22 (2007) 1287.
- [26] D. Buc, L. Stuchlikova, L. Harmatha, I. Hotovy, J. Mater. Sci.: Mater. Electron. 19 (2008) 783.
- [27] A. Ferhat Hamida, Z. Ouennoughi, A. Sellai, R. Weiss, H. Ryssel, Semicond. Sci. Technol. 23 (2008) 045005.
- [28] J.B. Casady, W. Johnson, Solid State Electron. 39 (1996) 1409.
- [29] T.P. Chow, V. Khemka, J. Fedison, N. Ramungul, K. Matocha, Y. Tang, R.J. Gutmann, Solid State Electron. 44 (2000) 277.
- [30] K. Kojima, H. Okumura, S. Kuroda, K. Arai, J. Cryst. Growth 269 (2004) 367.
- [31] K. Danno, T. Kimoto, K. Asano, Y. Sugawara, H. Matsunami, J. Electron. Mater. 34 (2005) 324.
- [32] K.S. Ramaiah, I. Bhat, T.P. Chow, J.K. Kim, E.F. Schubert, D. Johnstone, S. Akarca-Biyikli, J. Appl. Phys. 98 (2005) 106108.
- [33] W. Chen, K.Y. Lee, M.A. Capano, J. Cryst. Growth 297 (2006) 265.
- [34] K. Wada, T. Kimoto, K. Nishikawa, H. Matsunami, J. Cryst. Growth 291 (2006) 370.
- [35] K.S. Ramaiah, I. Bhat, T.P. Chow, J.K. Kim, E.F. Schubert, D. Johnstone, Physica B 391 (2007) 35.
- [36] O. Shigiltchoff, S. Bai, R.P. Devaty, W.J. Choyke, T. Kimoto, D. Hobgood, P.G. Neudeck, L.M. Porter, Mater. Sci. Forum 433–436 (2003) 705.
- [37] S.A. Reshanov, G. Pensl, K. Danno, T. Kimoto, S. Hishiki, T. Ohshima, H. Itoh, F. Yan, R.P. Devaty, W.J. Choyke, J. Appl. Phys. 102 (2007) 113702.
- [38] K.M. Geib, C. Wilson, R.G. Long, C.W. Wilmsen, J. Appl. Phys. 68 (1990) 2796.
- [39] F. Goesmann, R. Schmid-Fetzer, Mater. Sci. Eng. B 34 (1995) 224.
- [40] W.F. Seng, P.A. Barnes, Mater. Sci. Eng. B 72 (2000) 13.
- [41] J.P. Sullivan, R.T. Tung, M.R. Pinto, W.R. Graham, J. Appl. Phys. 70 (1991) 7403.
- [42] J.H. Werner, H.H. Güttler, J. Appl. Phys. 69 (1991) 1522.
- [43] R.T. Tung, Phys. Rev. B 45 (1992) 13509.
- [44] H.-J. Im, Y. Ding, J.P. Pelz, W.J. Choyke, Phys. Rev. B 64 (2001) 07310.
- [45] H. Benmaza, B. Akkal, H. Abid, J.M. Bluet, M. Anani, Z. Bensaad, Microelectron. J. 39 (2008) 80.
- [46] E.H. Rhoderick, R.H. Williams, Metal–Semiconductor Contacts, second ed., Clarendon, Oxford, 1988.
- [47] M.J. Bozack, Phys. Stat. Sol. (b) 202 (1997) 549.
- [48] S.M. Sze, Physics of Semiconductor Devices, Wiley–Interscience, 1981.
- [49] J. Osvald, Z.J. Horváth, Appl. Surf. Sci. 234 (2004) 349.
- [50] F. La Via, G. Galvagno, F. Roccaforte, A. Ruggiero, L. Calcagno, Appl. Phys. Lett. 87 (2005) 142105.
- [51] Y.P. Song, R.L. Van Meirhaeghe, W.H. Lafière, F. Cardon, Solid State Electron. 29 (1986) 633.
- [52] D.R. Lide, (Ed.), CRC Handbook of Chemistry and Physics, Internet Version 2005, <<http://www.hbcpnetbase.com>>, CRC Press, Boca Raton, FL, 2005.
- [53] M. Wiets, M. Weinelt, T. Fauster, Phys. Rev. B 68 (2003) 125321.
- [54] F. Giannazzo, F. Roccaforte, V. Raineri, S.F. Liotta, Europhys. Lett. 74 (2006) 686.
- [55] R.F. Schmitsdorf, T.U. Kampen, W. Mönch, J. Vac. Sci. Technol. B 15 (1997) 1221.
- [56] S. Chand, J. Kumar, J. Appl. Phys. 80 (1996) 288.
- [57] S. Chand, J. Kumar, J. Appl. Phys. 82 (1997) 5005.
- [58] A.N. Saxena, Surf. Sci. 13 (1969) 151.
- [59] N. Lundberg, M. Ostling, P. Tagtstrom, U. Jansson, J. Electrochem. Soc. 142 (1996) 1662.
- [60] L. Baud, C. Jaussaud, R. Madar, C. Bernard, J.S. Chen, M.A. Nicolet, Mater. Sci. Eng. B 29 (1995) 126.
- [61] O. Noblanc, C. Arnodo, S. Cassette, C. Brylinski, A. Kakanakova-Georgieva, T. Marinova, L. Kassamakova, R. Kakanakov, B. Pécz, A. Sulyok, G. Radnoczi, Mater. Sci. Forum 264–268 (1998) 817.
- [62] A. Kakanakova-Georgieva, T. Marinova, O. Noblanc, C. Arnodo, S. Cassette, C. Brylinski, Thin Solid Films 337 (1999) 180.
- [63] J. Kim, F. Ren, A.G. Baca, R.D. Briggs, S.J. Pearton, Solid State Electron. 47 (2003) 1345.
- [64] J. Kim, F. Ren, A.G. Baca, G.Y. Chung, S.J. Pearton, Solid State Electron. 48 (2004) 175.